

Rotational Spectrum of the AsH Radical in Its $a^1\Delta$ State, Studied by Far-Infrared Laser Magnetic Resonance¹

Rebecca A. Hughes,* John M. Brown,* and Kenneth M. Evenson†

*Physical and Theoretical Chemistry Laboratory, South Parks Road, Oxford OX1 3QZ, United Kingdom; and †National Institute of Standards and Technology, 325 Broadway, Boulder, Colorado 80303

Received May 2, 1997

The rotational spectrum of AsH in its metastable $a^1\Delta$ state has been recorded using a far-infrared laser magnetic resonance spectrometer. The AsH radical was produced inside the spectrometer by the reaction of arsine (AsH_3) with fluorine atoms. Hyperfine splittings from both ^{75}As and ^1H nuclei were observed, and analysis of the spectra yielded accurate values for rotational, hyperfine, and Zeeman parameters. © 1997 Academic Press

INTRODUCTION

This paper describes the rotational spectrum of AsH in the $a^1\Delta$ state, recorded by FIR laser magnetic resonance (LMR). The analysis of the measurements leads to the determination of accurate values for the rotational, hyperfine, and Zeeman parameters.

The molecule AsH is a Group V hydride, a close relative of the NH radical. As such, it has a $X^3\Sigma^-$ ground state with low-lying, reasonably metastable $a^1\Delta$ and $b^1\Sigma^+$ states. The ground state of the molecule is well characterized through studies at far-infrared (FIR) (1) and mid-infrared (2, 3) wavelengths. Information has also been obtained on the $b^1\Sigma^+$ state, from the direct observation of the $b^1\Sigma^+ - X^3\Sigma^-$ transition by Arens and Richter (4). On the other hand, almost nothing was known about the properties of AsH in the $^1\Delta$ state at the time we started the present study of its rotational spectrum in this metastable state.

During our work, a paper was published by Beutel *et al.* (5) who reported the detection of the $a^1\Delta - X^3\Sigma^-$ transition of AsH, observed in emission with a Fourier transform interferometer. They were able to determine the main parameters, namely T_e , B_e , D_e , ω_e , and $\omega_e x_e$, for AsH in the $a^1\Delta$ state. Previous theoretical calculations of AsH had predicted the $a^1\Delta$ state to lie at 9968 (6) or 8709 cm^{-1} (7) above the ground state; Beutel *et al.*, however, determined T_e to be smaller than these predictions, at 7216.84 cm^{-1} .

EXPERIMENTAL DETAILS

The FIR LMR spectrometer at the Boulder laboratory of NIST, which was used in this study, has been described elsewhere (8). The FIR radiation was generated in a chosen laser gas pumped by the appropriate line of an infrared CO_2 laser (see Table 1). Part of the FIR radiation was coupled

out of the laser cavity and detected with a liquid helium cooled Ga:Ge photoconductor detector. The resonance signals were modulated at 39 kHz using Zeeman modulation coils and amplified by a lock-in amplifier tuned to this frequency. The free radical AsH was formed in its metastable $^1\Delta$ state in the intracavity cell of the spectrometer by the reaction between fluorine atoms and arsine, AsH_3 . The atoms were formed by passing a 10% mixture of molecular fluorine in helium at 160 Pa (1.2 Torr) through a microwave discharge; the optimum pressure of AsH_3 was 1.33 Pa (10 mTorr). Laser lines with frequencies close to the transition frequencies of AsH in the $^1\Delta$ state calculated from the previously determined parameters for the $X^3\Sigma^-$ state (1, 3) were selected. The external magnetic field was scanned and spectra in both perpendicular ($\Delta M = \pm 1$) and parallel ($\Delta M = 0$) polarizations were recorded.

RESULTS AND ANALYSIS

Observations and Assignment

LMR spectra attributed to AsH in the $a^1\Delta$ state have been observed on four different laser lines whose details are given in Table 1. The rotational transitions have been assigned as $J = 3 \leftarrow 2$, $4 \leftarrow 3$, and $5 \leftarrow 4$ in the $^1\Delta$ state. The observations are summarized in the energy level diagram of Fig. 1. The detailed measurements are given, with their assignments, in Table 2. The assignment of the spectra was straightforward, based on the B and D values for the $X^3\Sigma^-$ state and on the linear Zeeman effect with $g_L = 1$. An example of the spectra is given in Fig. 2. It shows part of the 230.1 μm spectrum in perpendicular polarization. Two Zeeman components, $M_J = 1 \leftarrow 0$ and $M_J = -3 \leftarrow -2$, are marked; their first-order tuning rates are accidentally identical. Each shows a widely separated quartet structure, a manifestation of the ^{75}As hyperfine structure. The ^{75}As isotope, for which $I = \frac{3}{2}$, is the only naturally occurring isotope. Each line of this pattern is a

¹ Supported in part by NASA Contract W, 18-623.

TABLE 1
Details of the FIR Laser Lines Used to Record LMR Spectra
for AsH in the $a^1\Delta$ State

CO ₂ Laser line	Laser gas	Wavelength/ μm	Frequency/GHz ^a
9R42	CH ₂ F ₂	230.1	1302.8458
9R10	CH ₃ OH	232.9	1286.9995
10R20	¹³ CD ₃ OD	173.6	1726.5485
9R22	¹³ CH ₂ F ₂	138.3	2167.6912

^a Ref. (16)

closely spaced doublet arising from the ¹H hyperfine splitting. Many of the spectra showed signals attributable to other species. Two of these are AsH in its $X^3\Sigma^-$ state and AsH₂ in its \tilde{X}^2B_1 state. The latter can be identified from its hyperfine pattern, quartets of triplets (*ortho*) or singlets (*para*). Spectra for AsH in the $^3\Sigma^-$ and $^1\Delta$ states show similar hyperfine patterns but they can be easily distinguished in practice because the ⁷⁵As splitting is much larger for the $^1\Delta$ state. It is also worth noting that the optimum chemical conditions for the production of AsH are significantly different from those for the production of AsH₂; the latter requires a mixture which is richer in AsH₃.

Determination of Molecular Parameters

The measurements in Table 2 were used to determine the parameters of an effective Hamiltonian for a molecule in a $^1\Delta$ state:

$$H_{\text{eff}} = H_{\text{rot}} + H_{\text{hf}} + H_{\text{Zeem}}, \quad [1]$$

where

$$H_{\text{rot}} = BN^2 - D(N^2)^2 + H(N^2)^3, \quad [2]$$

$$H_{\text{hf}} = a_{\text{As}}\mathbf{I}_{\text{As}} \cdot \mathbf{L} + a_{\text{H}}\mathbf{I}_{\text{H}} \cdot \mathbf{L} + \text{eq}_0 Q(3I_{\text{As},z}^2 - \mathbf{I}_{\text{As}}^2)/[4I_{\text{As}}(2I_{\text{As}} - 1)], \quad [3]$$

and

$$H_{\text{Zeem}} = g'_L \mu_B B_0 L_Z - g_t \mu_B B_0 (N_Z - L_Z) + g_{\text{As}} \mu_N B_0 I_{\text{As},Z} + g_{\text{H}} \mu_N B_0 I_{\text{H},Z}. \quad [4]$$

The notation is standard and the various contributions are self-evident. Eq. [2] shows that the Hamiltonian is cast in the N^2 formulation. The data were fitted by a linearized, least-squares procedure using a computer program. The matrix representation of H_{eff} was truncated at $\Delta J = 2$ without loss in accuracy. Each measurement was given unit weight unless overlapped (weight of zero) or recorded with the 138.3 μm laser line (weight = 0.25). Resonances for this laser line occurred at high magnetic field and were very weak. Values for the parameters in Eqs. [2], [3], and [4] were determined

in the fit. The results are given in Table 2 (residuals) and Table 3 (parameter values). In the final fit, the sextic distortion parameter H was constrained to the value determined by Beutel *et al.* (5) since it agreed well with the value expected from the theoretical Dunham formula:

$$H_0 \simeq H_e = \frac{2}{3} D_e \left\{ 12 \left(\frac{B_e}{\omega_e} \right)^2 + \frac{\alpha_B}{\omega_e} \right\}. \quad [5]$$

The standard deviation of the fit, for a point of unit weight, was 0.7 MHz.

DISCUSSION

Pure rotational transitions have been detected in the AsH radical in its $a^1\Delta$ state and have been used to determine accurate rotational, hyperfine, and Zeeman parameters for this molecule. It is possible to compare the parameters of Beutel *et al.* (5) with ours, provided account is taken of the fact that they used an \mathbf{R}^2 formulation of the rotational Hamiltonian whereas we used the \mathbf{N}^2 version. Their values are given in Table 3; they are in good agreement with those determined in the present work but are much less precise. The rotational constant B_0 for AsH in the $^3\Sigma^-$ ground state is 215 884.54(48) MHz, slightly smaller than that for the $a^1\Delta$ state. The B_0 value in Table 3 can be combined with the α_B value from Ref. (5) (-6127 ± 18 MHz) to calculate a value for B_e of 219 828.4(90) MHz. This corresponds to a refined value for the equilibrium bond length r_e for AsH in the $^1\Delta$ state of 0.1 520 476(31) nm.

The hyperfine interactions for both ¹H and ⁷⁵As nuclei have been characterized for AsH in the $a^1\Delta$ state. The magnetic

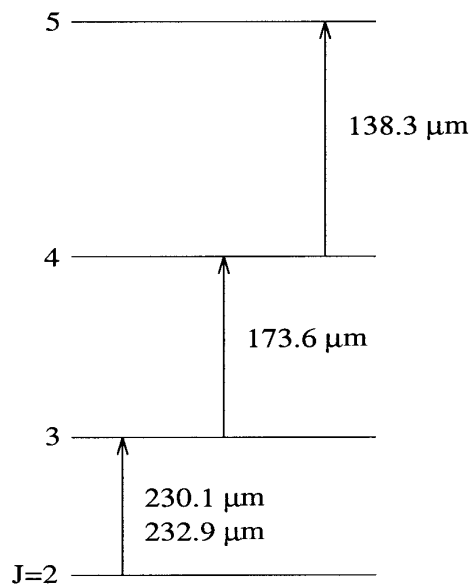


FIG. 1. The observed FIR transitions of $a^1\Delta$ AsH and the laser lines used to observe them.

TABLE 2
Details of the Observed Resonances in the Far-Infrared Spectrum
of AsH in the $v = 0$ Level of the $a^1\Delta$ State

J	M_J	$M_I(\text{As})^a$	$M_I(\text{H})^a$	ν_L (MHz)	B_0 (mT)	obs-calc (MHz)	$\partial\nu/\partial B_0$ (MHz/mT)
3 ← 2	2 ← 2	3/2	1/2	1286999.5	1267.69	-0.2	-9.21
			-1/2		1269.30	-0.1	-9.21
		1/2	1/2		1316.04	-1.0	-9.21
			-1/2		1317.65	-0.9	-9.21
		-1/2	1/2		1368.13	-0.9	-9.23
			-1/2		1369.73	-0.9	-9.23
	1 ← 2	3/2	1/2		1424.16 ^b	-1.7	-9.26
			-1/2		1425.70 ^b	-2.3	-9.26
		1/2	1/2		812.81	-0.7	-13.80
			-1/2		814.38	-1.1	-13.80
		-1/2	1/2		861.75	-1.1	-13.79
			-1/2		863.40	-0.4	-13.79
	0 ← 1	3/2	1/2		915.19	-0.5	-13.84
			-1/2		916.76	-0.8	-13.84
		1/2	1/2		973.47	-0.1	-13.96
			-1/2		975.04	-0.3	-13.96
		-1/2	1/2		1275.64	-0.3	-9.12
			-1/2		1277.25	-0.2	-9.12
3 ← 2	-2 ← -2	3/2	1/2	1302845.8	281.97	-0.6	9.42
			-1/2		283.56	-0.7	9.42
		1/2	1/2		324.54	-0.5	9.23
			-1/2		325.98 ^b	0.8	9.23
		-1/2	1/2		370.50	0.3	9.16
			-1/2		372.11	0.7	9.16
	-1 ← -1	3/2	1/2		418.07	1.2	9.17
			-1/2		419.68	1.1	9.17
		1/2	1/2		498.35	-0.6	4.76
			-1/2		630.03	-1.0	4.76
		-1/2	1/2		673.16	0.0	4.74
			-1/2		674.81 ^b	-0.3	4.74
	0 ← -1	3/2	1/2		721.90 ^b	0.1	4.73
			-1/2		723.54	-0.1	4.73
		1/2	1/2		774.51	0.4	4.74
			-1/2		776.08	0.5	4.74
		-1/2	1/2		281.40	-0.4	9.51
			-1/2		282.94	0.1	9.51
-3/2	1/2	1/2		322.73	0.1	9.35	
		-1/2		324.33	0.0	9.35	
	-1/2	1/2		368.82	-0.3	9.25	
		-1/2		370.38	0.0	9.25	
-3/2	1/2		418.45 ^b	0.3	9.15		
	-1/2		420.00	0.6	9.15		

^a The observed resonances obey the selection rule $\Delta M_I(\text{As})=0$, $\Delta M_I(\text{H})=0$.

^b Resonance overlapped by that of another species; measurement given zero weight in the fit.

^c Proton hyperfine structure not resolved.

^d Measurement given a weight of 0.25 in the fit (corresponds to an experimental uncertainty of 3 MHz).

TABLE 2—Continued

J	M_J	$M_I(\text{As})^a$	$M_I(\text{H})^a$	ν_L (MHz)	B_0 (mT)	obs-calc (MHz)	$\partial\nu/\partial B_0$ (MHz/mT)
3 ← 2	1 ← 0	3/2	1/2	1302845.8	623.93	0.6	4.78
			-1/2		625.55	0.5	4.78
		1/2	1/2		667.95	-0.2	4.76
			-1/2		669.59	-0.5	4.76
		-1/2	1/2		718.13	0.6	4.76
			-1/2		719.74	-0.6	4.76
	-3 ← -2	3/2	1/2		775.82	-0.9	4.77
			-1/2		777.46	-1.2	4.77
		1/2	1/2		627.58	-0.8	4.62
			-1/2		629.21	-0.9	4.62
		-1/2	1/2		680.43	-0.4	4.61
			-1/2		682.08	-0.7	4.61
4 ← 3	3 ← 3	3/2	1/2	1726548.5	817.23	0.3	-5.47
			-1/2		818.86	0.5	-5.47
		1/2	1/2		868.56	0.1	-5.47
			-1/2		870.17	0.2	-5.47
		-1/2	1/2		923.92	0.6	-5.51
			-1/2		925.47	0.3	-5.51
	2 ← 2	3/2	1/2		983.07	0.6	-5.58
			-1/2		984.77	1.2	-5.58
		1/2	1/2		1277.45	1.2	-3.67
			-1/2		1279.15	1.6	-3.67
		-1/2	1/2		1328.65	0.9	-3.68
			-1/2		1330.35	1.3	-3.68
5 ← 4	-3 ← -3	3/2	^c	2167691.2	1695.44 ^d	-4.8	2.84
			1/2		1741.92 ^d	-4.7	2.84
		-1/2	^c		1790.27 ^d	-4.8	2.84
	-3/2	^c	1840.34 ^d		-4.7	2.84	

and electronic hyperfine parameters for the first three Group V diatomic hydrides in the $^1\Delta$ state are summarized in Table 4. The nuclear spin electron orbital interaction parameter a_α depends on the inverse cube of the separation between the open shell electrons i and the nucleus in question, α ,

$$a_\alpha/\text{MHz} = \left(\frac{10^{-6}}{h}\right) \left(\frac{2\mu_B g_N \mu_N}{4\pi\mu_0^{-1}}\right) \sum_i \langle 1/r_{i\alpha}^3 \rangle_l, \quad [6]$$

where the notation is standard. The $\langle 1/r_{i\alpha}^3 \rangle_l$ values for both As and H, which have been determined from our work, are also given in Table 4, along with the corresponding parameters for NH and PH. The π orbital which contains the two open shell electrons is predominantly

X (np) in character. If we compare the experimentally determined value with that for the X atom in an np orbital, which has been calculated *ab initio* (see Table 4), we see that these two values are similar. It can thus be seen that, although the representation of the π orbital by an np atomic orbital is rather naive, it is nevertheless quite accurate. Turning our attention to the proton parameter, we note that the interaction arises from the two $np\pi$ electrons centered on the X atom. Therefore we expect $\langle 1/r_{i\alpha}^3 \rangle$ to be well approximated by $1/r^3$ where r is the XH bond length. This expectation is borne out in practice as can be seen in Table 4. The ^{75}As splittings also have a contribution from the electric quadrupole coupling term. The value determined for the $a^1\Delta$ state, $-124.1(18)$ MHz, is slightly larger than the correspond-

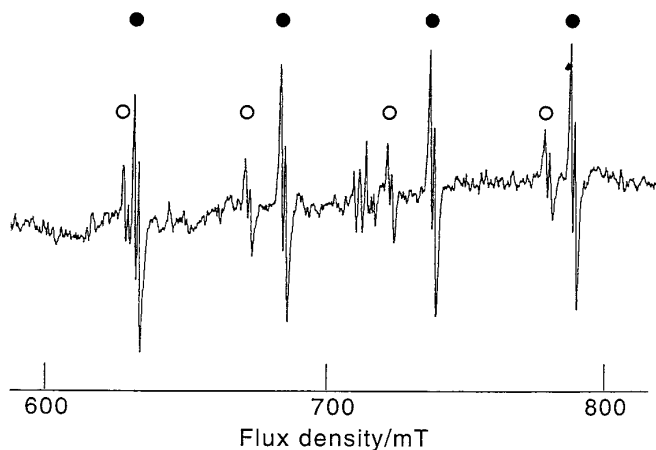


FIG. 2. A portion of the FIR spectrum recorded on the 230.1 μm laser line in perpendicular polarization. The $M_J = 1 \leftarrow 0$ and $-3 \leftarrow -2$ transitions are labeled by \circ and \bullet , respectively. The large quartet splitting arises from the ^{75}As hyperfine interactions and the much smaller doubling from the ^1H hyperfine structure. The two sets of M_J transitions overlap because their first-order tuning rates are accidentally the same.

ing parameter for the $^3\Sigma^-$ state, $-95.6(39)$ MHz. This implies that the electric field gradient at the As nucleus is slightly larger in the $^1\Delta$ state.

An analysis of the Zeeman parameters also provides information on the electronic structure of AsH in the $a^1\Delta$ state. The orbital g -factor g_L^1 is given by

$$g_L^1 = 1.0000 - \delta g + \Delta g_L, \quad [7]$$

where δg is the relativistic correction and Δg_L is the nonadiabatic correction term (12). Using $\delta g = 1 \times 10^{-4}$, we obtain a value for Δg_L of $1.339(16) \times 10^{-3}$.

The rotational g -factor g_r has separate contributions from rotation of the bare nuclei and the electrons:

$$g_r = g_r^N - g_r^e. \quad [8]$$

The nuclear contribution (g_r^N) can be estimated from simple magnetostatics (13),

$$g_r^N = \left(\frac{m_e}{m_1 + m_2} \right) \left(\frac{Z_1 m_2^2 + Z_2 m_1^2}{m_1 m_2} \right), \quad [9]$$

where m_i and Z_i are the masses and charges of the two nuclei and m_e is the mass of the electron. This expression gives $g_r^N = 5.40 \times 10^{-4}$ for $^{75}\text{As}^1\text{H}$. Using the fitted value for g_r of $-7.32(16) \times 10^{-4}$, we find $g_r^e = 1.272 \times 10^{-3}$. This parameter measures the combined effects of the admixture of $^1\Pi$ and $^1\Phi$ states into the $a^1\Delta$ state (12). Its value is consistent with the corresponding value

for ND, $1.13(10) \times 10^{-3}$, since it should be proportional to the B -value given the same disposition of electronic states (for ND, $B_0 = 264.750$ GHz, and for AsH, $B_0 = 216.765$ GHz).

Whereas the parameter g_r^e depends on the sum of its contributions from the admixture of excited $^1\Pi$ and $^1\Phi$ states, the parameter Δg_L depends on the *difference* of the same contributions. If the effects of admixture of $^1\Pi$ states outweigh those of the $^1\Phi$ states, the two parameters are related by

$$g_r^e = 2\Delta g_L. \quad [10]$$

This relationship is not well obeyed in the case of AsH, suggesting that there may be a significant contribution to the parameters from the mixing with $^1\Phi$ states as well as with $^1\Pi$ states. However, the relationship does hold very well for both NH (9) and OH⁺ (14) in their $^1\Delta$ states and the general disposition of electronic states is expected to be very similar for all Group V diatomic hydrides. It therefore seems more likely that deviation from the relationship in Eq. [10] in the case of AsH is attributable to the increasing effects of spin-orbit coupling as one goes down a group in the periodic table. Such mixing can be treated by third-order perturbation theory and modifies the orbital g -factor (15). The effect is particularly marked if one of the atoms is heavy.

TABLE 3
Molecular Parameters for ^{75}AsH in the $v = 0$ Level of the $a^1\Delta$ State, Determined by a Least-Squares Fit of the Far-Infrared LMR Spectrum

Parameter ^a	Value	Other work ^b
B_0	216 764.960(50) ^c	216 764(1)
D_0	9.8 837(20)	9.88(1)
$10^3 H_0$	0.21 ^d	0.21(2)
a_{As}	703.54(15)	
a_H	22.34(35)	
$(eQq_0)_{As}$	-124.1(18)	
g_L^1	1.001 239(16)	
$10^3 g_r$	-0.732(16)	
$g_N(\text{As})$	0.95 965 ^d	
$g_N(\text{H})$	5.58 569 ^d	

^a Value in MHz (where appropriate).

^b Values determined by Beutel *et al.* (5), converted from \mathbf{R}^2 to \mathbf{N}^2 formulation for comparison with the present work.

^c The numbers in parentheses represent one standard deviation of the least-squares fit, in units of the last quoted decimal place.

^d Parameters constrained in the fit.

TABLE 4
Hyperfine and Derived Parameters for Group V Hydrides, XH, in the $a^1\Delta$ State

X	a_X MHz	a_H MHz	$(eQq_0)_X$ MHz	$\langle r_i^{-3} \rangle_X^a$ 10^{30} m^{-3}	$\langle r_i^{-3} \rangle_X^b$ 10^{30} m^{-3}	$\langle r_i^{-3} \rangle_H^c$ 10^{30} m^{-3}	$r_0^{-3}(\text{XH})^d$ 10^{30} m^{-3}
$^{14}\text{N}^e$	109.65(85)	70.9(14)	-4.0(15)	19.3	24.29	0.89	0.8784
$^{31}\text{P}^f$	768(37)	28(15)	- ^g	23.7	28.62	0.3	0.3399
^{75}As	703.54(15)	22.34(35)	-124.1(18)	51.852	61.42	0.2829	0.2786

^a For X in XH molecule, calculated from a_X .

^b For atomic X, obtained from Herman and Skillman's wavefunction (11).

^c For H in XH molecule, calculated from a_H .

^d Calculated from $B_0(\text{XH})$.

^e Ref. (9)

^f Ref. (10)

^g ^{31}P has a nuclear spin of 1/2 and so does not show an electric quadrupole coupling.

ACKNOWLEDGMENTS

R.A.H. thanks the Physical and Theoretical Chemistry Laboratory (PTCL), Jesus College, Oxford, and the National Institute of Standards and Technology (NIST), Boulder, for financial support.

REFERENCES

1. K. Kawaguchi and E. Hirota, *J. Mol. Spectrosc.* **106**, 423–429 (1984).
2. J. R. Anaconda, P. B. Davies, and S. A. Johnson, *Mol. Phys.* **56**, 989–993 (1985).
3. K. D. Hensel, R. A. Hughes, and J. M. Brown, *J. Chem. Soc. Faraday Trans.* **91**, 2999–3004 (1995).
4. M. Arens and W. Richter, *J. Chem. Phys.* **93**, 7094–7096 (1990).
5. M. Beutel, K. D. Setzer, O. Shestakov, and E. H. Fink, *J. Mol. Spectrosc.* **178**, 165–171 (1996).
6. T. Matsushita, C. Marian, R. Klotz, and S. D. Peyerimhoff, *Can. J. Phys.* **65**, 155–164 (1987).
7. K. Balasubramanian and V. Nannegari, *J. Mol. Spectrosc.* **138**, 482–486 (1989).
8. T. J. Sears, P. R. Bunker, A. R. W. MacKellar, K. M. Evenson, D. A. Jennings, and J. M. Brown, *J. Chem. Phys.* **77**, 5348–5362 (1982).
9. K. R. Leopold, K. M. Evenson, and J. M. Brown, *J. Chem. Phys.* **85**, 324–330 (1986).
10. P. B. Davies, D. K. Russell, D. R. Smith, and B. A. Thrush, *Can. J. Phys.* **57**, 522–528 (1979).
11. F. Herman and S. Skillman, "Atomic Structure Calculations," p. 346, Prentice-Hall, Englewood Cliffs, NJ, 1963.
12. J. M. Brown and H. Uehara, *Mol. Phys.* **24**, 1169–1174 (1972).
13. A. Carrington, D. H. Levy, and T. A. Miller, *Adv. Chem. Phys.* **18**, 149–248 (1970).
14. T. D. Varberg, K. M. Evenson, and J. M. Brown, *J. Chem. Phys.* **100**, 2487–2491 (1994).
15. J. M. Brown, C. R. Byfleet, B. J. Howard, and D. K. Russell, *Mol. Phys.* **23**, 457–468 (1972).
16. N. G. Douglas, "Millimetre and Submillimetre Wavelength Lasers," Springer-Verlag, Berlin, 1989.